Rev. Roum. Sci. Techn.– Électrotechn. et Énerg.
Vol. **63**, *3*, pp. 306–313, Bucarest, 2018

STANDALONE ANALOG ACTIVE CELL-BALANCING CIRCUIT FOR AUTOMOTIVE BATTERY MANAGEMENT SYSTEMS

BOGDAN ANTON, ADRIANA FLORESCU, ŞTEFAN GEORGE ROŞU

Key words: Active balancing circuit, Battery management system, Boost converter, Charging circuit, Lithium-ion cells, Plug-in hybrid electric vehicles.

This paper presents a standalone analog active balancing circuit designed for series-connected Lithium-ion cells, which can be used together with an automotive battery management system (BMS). A very important parameter of the charging circuit, especially when it's used for plug-in hybrid electric vehicles (PHEVs) or electric vehicles (EVs) is its efficiency, which affects both the capacity of the battery pack and its lifespan. Our proposed design is simple, derived from a boost converter and can be used either as a fully analog standalone circuit or it can be interconnected with microcontrollers or processors. In addition to this, another advantage over some different approaches is the ability of balancing the series-connected lithium-ion batteries during both charging phase and discharging phase, increasing their available capacity and preventing uneven and over-discharging for different cells. The proposed architecture was tested and validated using both simulation software and practical hardware implementation revealing that the obtained results were very similar to the initial expectations and calculations.

1. INTRODUCTION

Lithium based batteries are being used more and more often, mainly because of the electrification and hybridization of vehicles, as well as due to the need of transitioning to eco-friendly energy storage systems, therefore the relatively high demand of instantaneous power can only be achieved by connecting tens or hundreds of batteries in series or in a series-parallel configuration [1, 2], since the nominal voltage of each cell doesn't exceed 4 V.

Considering this, special attention should be paid to the balancing circuit, which is a part of the BMS, otherwise the entire battery pack may fail and damage the surrounding components and devices, due to overtemperature stress, discharging below the safe limit or overcharging.

Apart from these failure mechanisms which may occur, the unbalance between cells causes a decrease of capacity for the entire pack, reducing both the reliability and the total useful energy stored within.

To achieve even charging voltages (which translates into equal amount of stored energy) for all cells, while they are connected in series, there are several methods which rely either on using passive (dissipative) circuits or using active (non-dissipative) circuitry, both having advantages and drawbacks when it comes to efficiency, complexity, reliability and costs [3].

Depending on the application, one of the two categories may be suitable, taking into account the amount of power needed to charge the batteries and also how often they will be used. Furthermore, stationary battery packs may not have efficiency and space constraints, while the packs used for EVs and hybrid electric vehicles (HEVs) or PHEVs may suffer from this shortcoming. Considering this, the need for efficient heat removal (which is produced by the cells and balancing circuitry during charging and discharging phases) is very high, therefore optimal dimensioning may be required [4–6], as well as performance estimation [7].

This article aims to provide a hybrid solution (combining active and passive balancing circuitry, in a very efficient configuration), intended to overcome some drawbacks found in several other approaches, such as the complexity and costs added by the use of a transformer [8–11], as well as presenting the results obtained for the practical implementation of the proposed architecture.

On the other hand, compared to [12, 13], which present some solutions that allow energy transfer between any cell within the string (but in the same time, the complexity of their circuitry is increased), this architecture is simple, based on neighbor-only energy transfer.

Our proposed design is meant to utilize a reduced number of switching devices, similar to [5], and relies on voltage-based cell-balancing, rather than prediction and relative capacity estimation algorithms [10].

In contrast to other papers [9, 14], that propose some active balancing circuits capable of equalizing the voltage across each cell within the battery pack during charging phase only, our design is able to balance the voltages during discharge phase, also, contributing to a better exploitation of the useful energy stored within the pack and preventing the worn-out cells to over-discharge.

Moreover, every module consisting of several series-connected or series-parallel-connected cells can be either used as a standalone or decentralized unit, as proposed in [14] or they can require some sort of global coordination, being able to communicate as master and slave with the BMS or other equipment [15], such as computers or portable devices [16]. This feature allows for real-time state of charge (SOC) and voltage monitoring of the battery pack [17], as well as error reporting in case of failure occurrence, therefore extending the existing list of parameters used for vehicles diagnostics [18], when it comes to HEVs or PHEVs.

This paper focuses on providing a simple alternative to the commonly used cell-balancing circuits and it is organized as follows:

- Section 2 presents a comparison between different types of cell-balancing circuits, together with our proposed architecture.
- Section 3 reveals the simulation results which were performed on a particular example, consisting of four series-connected lithium-ion cells.
- Section 4 aims to validate the simulation results, comparing them with real measurements, which

"Politehnica" University of Bucharest, Faculty of Electronics, Telecommunications and Information Technology, Bd. Iuliu Maniu, Nr. 1-3, Sector 6, Romania., bogdan_anton_2005@yahoo.com

were obtained after the hardware implementation of the standalone analog circuitry.

- Section 5 highlights the conclusions of this work, disclosing also some future development directions intended to improve both the performances and the accuracy of the proposed active cell-balancing circuit architecture that can be used for automotive BMSs, mainly due to its high efficiency and low complexity.

2. CELL-BALANCING DESIGN

There are several designs of cell-balancing circuits for rechargeable batteries in the literature, but, from the power dissipation standpoint, they can be split into two main categories: dissipatives (or passives) and non-dissipatives (or actives).

The first category (presented in Fig. 1) uses 'bleeding' resistors, which dissipate the excess power for a certain cell from a string, when one of them is over-charged, compared to the others.

Because the cells which compose the battery pack are connected in series or in a series-parallel configuration and charged all together, this technique allows to deflect a part of the charging current through the resistive load, therefore the voltage across each cell will be maintained at a safe and regulated value.

The main advantages of this design are represented by its cost and complexity, but on the other hand, the efficiency is poor, meaning that the balancing circuitry needs to be located far from the cells, due to the amount of heat generated, which may cause damage.

The second category, which uses non-dissipative (or active) cell-balancing techniques, can be divided into two sub-categories, depending on the storage element: capacitives and inductives.

An example of capacitive active cell-balancing circuit is presented in Fig. 2, where the energy is redistributed from one cell to the other through a capacitor. However, the efficiency of this circuit is only 50 % [19], which translates into high amount of losses, especially when used for tens or hundreds of series (or series-parallel) connected rechargeable batteries.

The second subcategory of active cell-balancing circuits uses inductive-based switched-mode dc-dc (direct current-direct current) converters to transfer in a very efficient way the energy from one cell to another.

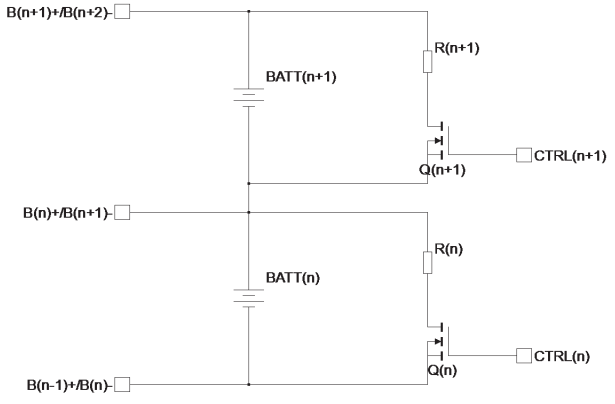

Fig. 1 – Example of a passive cell-balancing circuit using 'bleeding' resistors.

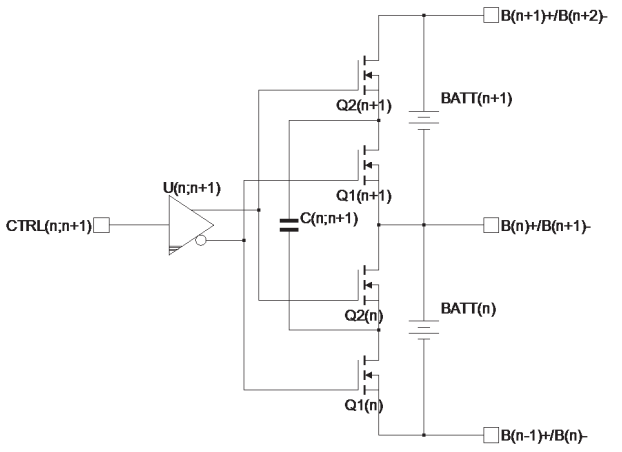

Fig. 2 – Example of an active cell-balancing circuit using switched capacitors.

One example of this type of power converters is shown in Fig. 3 and it's based on the buck-boost topology, which allows the output voltage to be either higher or lower than its input voltage, but in the same time the polarity is inverted, which does not necessarily represent an issue for this kind of applications.

However, the main drawbacks of this approach are introduced by significant developing and production costs for the circuitry, as well as its high level of complexity.

A variation of this active balancing circuit is proposed in this article (Fig. 4) and the principle of operation is based on the transfer of the excess energy from the lower cell to the upper neighbor cell, in contrast to the previous example (Fig. 3), which allows the transfer from the upper battery to the lower battery.

The main advantage of this topology (which is actually a non-synchronous boost converter with the load connected between its output and input, performing the same function as a non-inverting buck-boost converter) consists in placing the switching transistor with its gate referenced to a virtual ground, therefore, it can be driven directly, without the need of a high-side MOSFET driver.

When used in its normal configuration (with the load connected between the output and the ground reference), the boost converter produces a regulated output voltage greater in magnitude than the input voltage. In order to extend the output voltage range to either lower or higher values than the input, the load should be connected as described in the previous paragraph, therefore the boost converter being able to perform the function of a buck-boost converter.

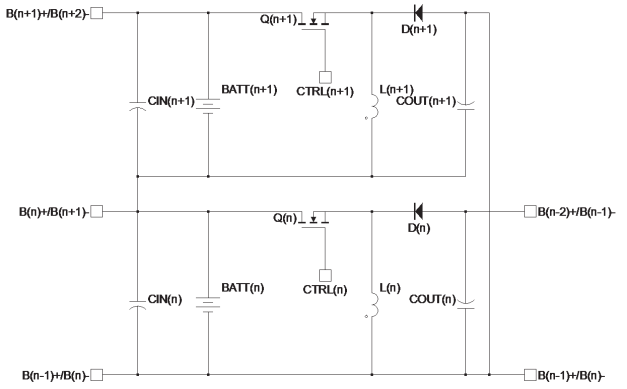

Fig. 3 – Example of an active cell-balancing circuit using inverting buck-boost switching regulators.

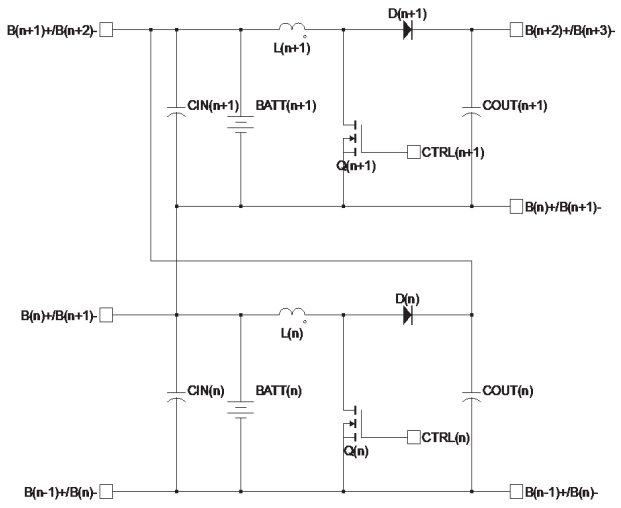

Fig. 4 – Example of an active cell-balancing circuit using boost converters working as non-inverting buck-boost switching regulators.

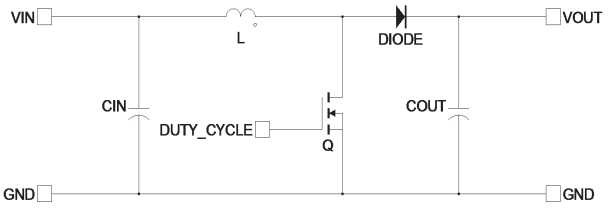

Fig. 5 – Schematic of the power train for the non-synchronous boost converter.

In order to determine the voltage conversion ratio of the boost converter (which is presented in Fig. 5), as a function of the duty cycle, D, its steady-state operation in continuous conduction mode (CCM) will be analyzed according to [20], assuming that every electronic component is ideal (the voltage across the diode and transistor, Q, are zero) and ignoring the ac (alternating current) ripple across the capacitors.

Knowing the inductor current waveform, the inductor voltage can be found by use of (1):

$$V_L = L\frac{\Delta I_L}{\Delta t}, \tag{1}$$

where L is the inductance, ΔI_L is the change in current and Δt is the length of the subinterval.

During ON state, because the transistor is saturated, the voltage across the inductor will be equal to the voltage of the input supply, therefore it can be expressed by using (2):

$$V_{IN} = L\frac{\mathrm{d}I_{L_{ON}}}{\mathrm{d}t}. \tag{2}$$

Thus, during the first interval, the slope of the inductor current waveform is given by (3):

$$\Delta I_{L_{ON}} = \frac{1}{L}\int_0^{DT} V_{IN}\,\mathrm{d}t = \frac{DT}{L}V_{IN}, \tag{3}$$

where T is the switching period.

During OFF state, because the transistor is in the cut-off region, the voltage across the inductor will be equal to the difference between the voltage of the input supply and the output voltage, therefore it can be expressed by using (4):

$$V_{IN} - V_{OUT} = L\frac{\mathrm{d}I_{L_{OFF}}}{\mathrm{d}t}. \tag{4}$$

Thereby, during the second interval, the slope of the inductor current waveform is given by (5):

$$\Delta I_{L_{OFF}} = \int_{DT}^{T}\frac{\left(V_{IN}-V_{OUT}\right)}{L}\mathrm{d}t = \frac{\left(V_{IN}-V_{OUT}\right)\left(1-D\right)T}{L}. \tag{5}$$

Since, in steady-state, the total volt-seconds applied over one switching period must be zero, this means that the overall change in the current is also zero, leading to (6), (7):

$$\Delta I_{L_{ON}} + \Delta I_{L_{OFF}} = 0 \tag{6}$$

$$\frac{V_{IN}DT}{L} + \frac{\left(V_{IN}-V_{OUT}\right)\left(1-D\right)T}{L} = 0. \tag{7}$$

Assuming this, the voltage conversion ratio for the boost converter can be expressed by use of (8):

$$\frac{V_{OUT}}{V_{IN}} = \frac{1}{1-D}. \tag{8}$$

For the topology proposed in this article, the load will be connected between the output and the input of the converter, as previously mentioned. This approach allows for obtaining a broader range of output voltage, which translates into a higher level of flexibility.

Considering the example given in Fig. 4, the input voltage for each boost converter is represented by the nominal voltage of each battery, BATT(n) or BATT(n + 1), while the output voltage (referenced to the negative terminal of the first cell) is delivered to both cells connected in series. Since BATT(n) and BATT(n + 1) are almost identical, the output voltage of the converter should have twice the magnitude of one cell, therefore, the duty cycle should be approximately 0.5. On the other hand, assuming that the load of the first regulator is represented by BATT(n + 1), the voltage drop across it will be equal to the voltage drop across BATT(n).

3. SIMULATION RESULTS

All the simulations presented in this chapter were performed using SIMPLIS, which is a simulation tool dedicated to analog switched mode power supplies (SMPSs). Figure 6 reveals the simplified schematic of the proposed cell-balancing circuit, together with the charger and four batteries. All the circuitry consists of a power supply (V4), one passive balancing circuit (consisting of R15, Q1, R2, V1 and S1, which acts as a switch with integrated comparator) and three switching regulators, along with all the additional components required for a proper operation (switches with integrated comparators for enabling and disabling the devices, as well as waveform generators for the driving signals).

The power source which feeds the series-connected string of batteries consists of an ideal dc power supply, together with a circuit which limits the charging current of the cells to a predetermined value (consisting of the operational amplifier X1, two voltage references, V2 and V10, as well as R4, C8 and C11). During the simulations, the charging current was chosen to be 300 mA.

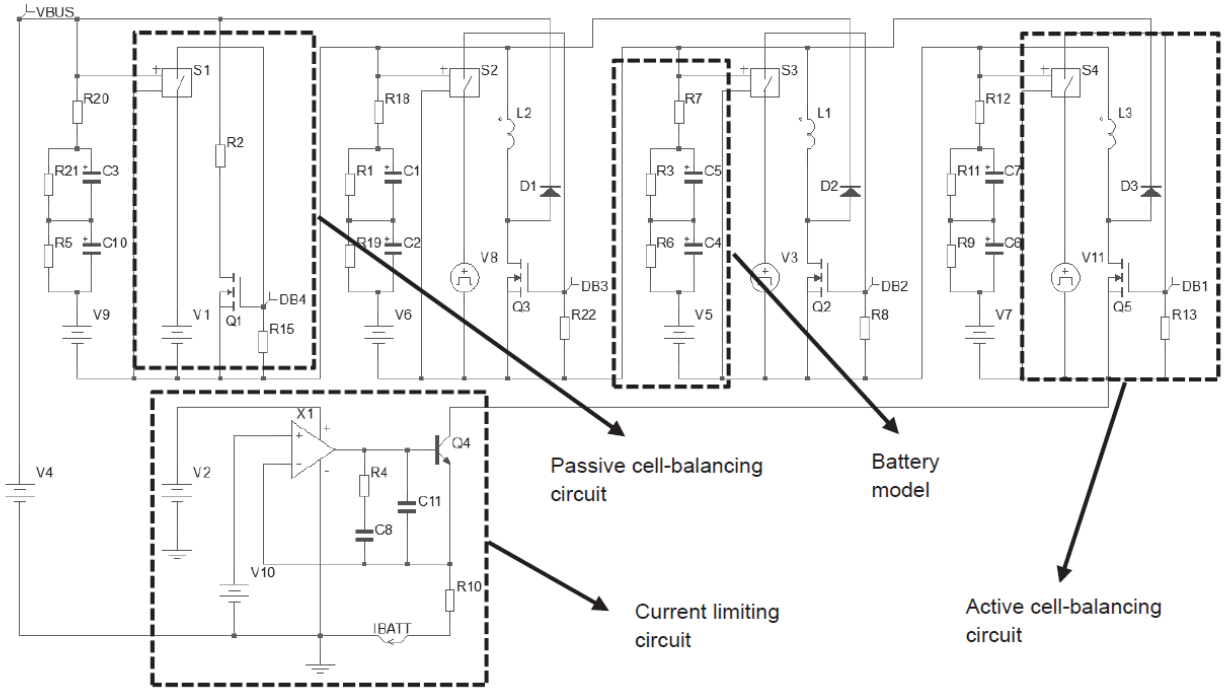

Fig. 6 – Simplified schematic of the cell-balancing circuit used for simulation.

For simplicity reasons, the string of serially-connected lithium cells was reduced to 4 (during simulations), therefore the proof of concept for the proposed analog active cell-balancing circuit could be easily simulated, implemented and validated. On the other hand, considering that in real applications this balancing circuit will be used for many series-connected cells (for example, 50 cells [1, 2], or more), just the last one uses a passive (dissipative) method of balancing, for cost and complexity reasons, but still without compromising the overall efficiency of the BMS. If this solution is considered to be less effective than needed, a transformer-based active cell-balancing circuit can be used, allowing the energy transfer from the last cell to the first one.

Each cell was designed based on a two-time constants model [21], as shown in Fig. 7 and each of the dc-dc converters were operated in open-loop, with a fixed duty cycle, calculated based on the targeted charging voltage for every battery. According to [21], the description in discrete time for each cell is given by (9), (10) and (11):

$$v_{1,k+1} = v_{1,k} e^{\frac{-Ts}{\tau_1}} + R_1 \left(1 - e^{\frac{-Ts}{\tau_1}}\right) i_{Batt,k}, \qquad (9)$$

$$v_{2,k+1} = v_{2,k} e^{\frac{-Ts}{\tau_2}} + R_2 \left(1 - e^{\frac{-Ts}{\tau_2}}\right) i_{Batt,k}, \qquad (10)$$

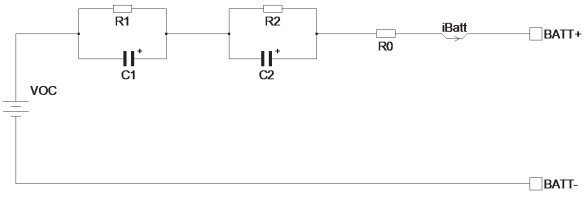

Fig. 7 – Example of a two-time constants model for a lithium-ion battery.

$$v_{Batt,k} = V_{OC}\left(SOC_k\right) - v_{1,k} - v_{2,k} - R_0 i_{Batt}, \qquad (11)$$

where k and $k + 1$ are two consecutive samples, T_S is the sampling period, τ is the RC time constant, R_0 is the internal resistance, V_{OC} is the open-circuit voltage, v_{Batt} is the voltage across the entire battery model and i_{Batt} is the value of the current flowing through the R_0. For our proposed example, the short time transient behavior was chosen around to be 20 ms for each cell, while the long time transient behavior was chosen to be around 2 s (because of the constraints introduced by the simulation time).

Figure 8 reveals the output voltage for each cell (VB1, VB2, VB3 and VB4) during charging and balancing phases, which has a threshold set to 4.15 V, with 60 mV (± 30 mV) hysteresis.

Because the simulator requires a large amount of hardware resources when running complex schematics, the decision was to reduce the simulation time to 10 s, as well as adjusting the charging current accordingly (300 mA, as mentioned before). In addition to this, the simulation started with initial

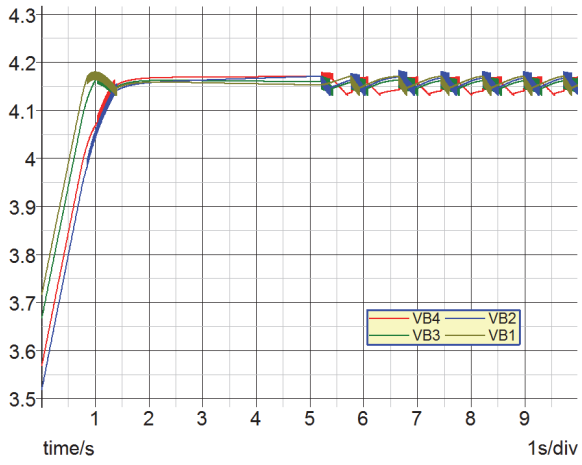

Fig. 8 – Simulation waveforms for the series-connected lithium cells during the charging and balancing phases.

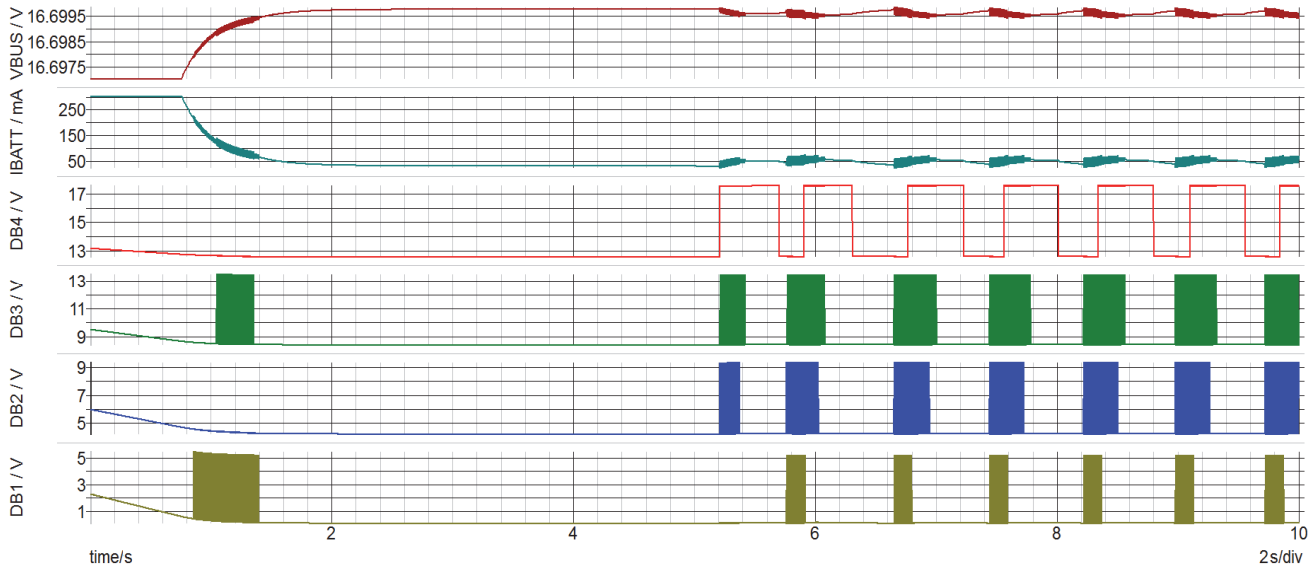

Fig. 9 – Simulation waveforms for the series-connected cells during the charging and balancing phases.

conditions and the batteries were pre-charged to different voltage levels (from 3.525 V to 3.725 V), in order to point out the natural unbalance of the cells and to demonstrate the functionality of the proposed architecture.

Figure 9 discloses the waveforms for different parameters (which were monitored during charging and balancing phases), such as the voltage across the entire string of cells (VBUS) or the current which flows through them (IBATT), as well as the driving signals for each balancing circuit (DB1, DB2, DB3 and DB4).

Because the current limiting circuit (which was designed using both the bipolar junction transistor (BJT), Q4, and the shunt R10) is connected in series with the rechargeable batteries, the voltage applied is around 17 V.

Regarding the control voltages for both the active cell-balancing circuits (DB1, DB2 and DB3), as well as for the passive cell-balancing circuit (DB4), they have an amplitude of around 5 V and are floating with regards to the ground reference.

The main advantage of the architecture proposed in this paper is that the voltage across each of the batteries is balanced even during discharging phase, which conducts to a more effective utilization of the energy stored inside the entire pack and helps avoiding over discharge for every cell.

As an extra benefit, this approach can be also used to charge and balance super-capacitors, with minimum hardware changes.

4. PRACTICAL IMPLEMENTATION

For the practical implementation of the proposed balancing circuit, Altium Designer tool was used. The block diagram of the implemented cell-balancing circuit is shown in Fig. 10, while the schematic for the battery charger, which is a single-ended primary-inductor converter (SEPIC) designed using a low side pulse width modulation (PWM) controller is presented in Fig. 11.

The SEPIC topology was chosen for two main reasons: it offers inherited short-circuit protection, since its input is separated from the output through the coupling capacitor (C3) and also because the output voltage (which has the same polarity as the input) can be either higher or lower than the input voltage, thus offering flexibility regarding the power supply. On the other hand, the front-end converter is configured to work as a constant-current, constant-voltage battery charger.

The four series-connected balancing circuits consist of three active circuits (implemented using non-synchronous fixed frequency boost switching regulators) and one passive circuit (for complexity reasons). A part of the balancing circuit (consisting of one passive and one active cell-balancing circuit) is shown in Fig. 12.

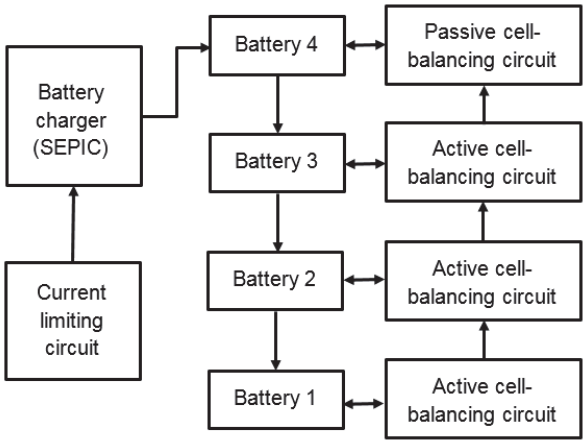

Fig. 10 – Block diagram of the implemented cell-balancing circuit.

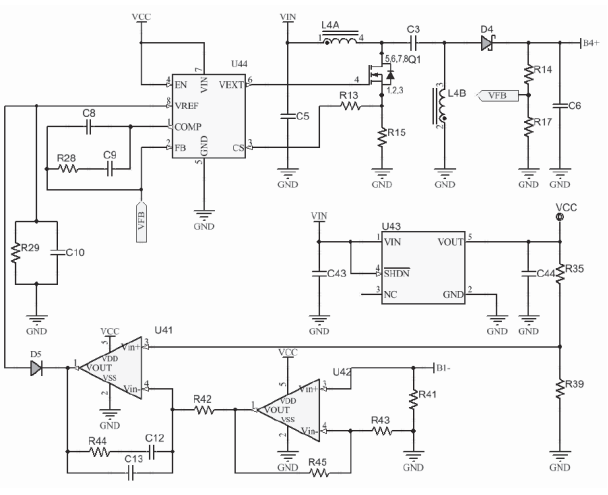

Fig. 11 – Schematic of the implemented SEPIC battery charger.

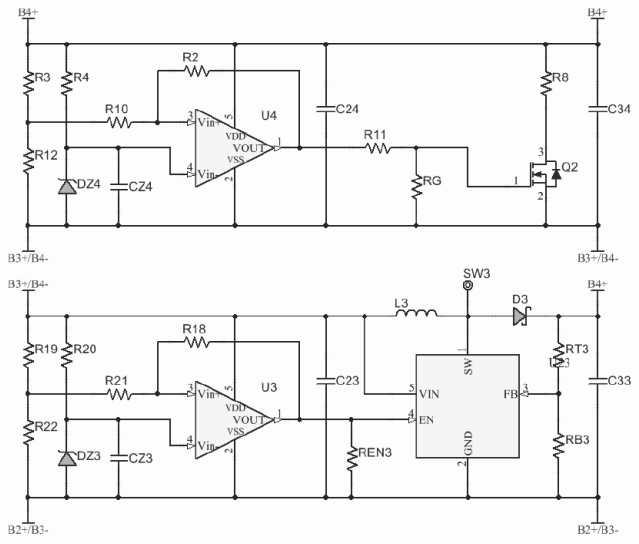

Fig. 12 – Schematic of two cell-balancing circuits (passive on the top and active on the bottom) used for the hardware implementation.

For simplicity, each comparator (U3 and U4) used for the balancing circuit is supplied from its corresponding cell and utilizes a 2.4 V Zener diode as a voltage reference. However, this approach has some limitations regarding the precision (the voltage varies with temperature). Moreover, the switching regulators are also supplied from the batteries, working as floating circuits, allowing in the same time the use of low voltage devices, which are usually more affordable.

When the voltage drop across a particular cell reaches 4.18 V (because the threshold set to 4.15 V has a hysteresis of ± 30 mV), its corresponding cell-balancing circuit starts to redistribute the excess energy to the upper rechargeable battery until the threshold of 4.12 V has been reached. This mechanism applies for all batteries that are connected to an active cell-balancing circuitry.This solution offers flexibility, because it utilizes analog components which can be either linked to a microprocessor unit (MPU) inside the BMS or they can be left working as a standalone circuitry, with minor hardware changes.

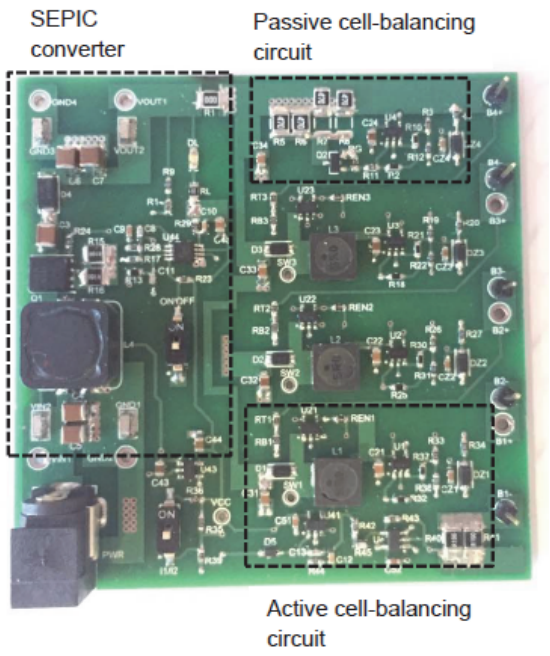

Fig. 13 – Overview of the hardware implementation, consisting of the battery charger, 3 active cell-balancing circuits and one passive cell-balancing circuit.

Regarding the last cell from the top of the string, its corresponding balancing circuitry uses a passive architecture, since it cannot redistribute the excess energy to another upper cell and the transfer to the first cell implies increasing the complexity of the entire design. However, the comparator uses the same thresholds as the rest of them (utilized for the three active circuits), meaning that it enables the passive circuit when the voltage across the battery reaches 4.18 V and disables it when the voltage falls below 4.12 V.

After selecting four used lithium-ion batteries (each of them featuring a nominal capacity of 2 200 mAh and being charged at different voltage levels), they had been connected to the charging and balancing circuitry revealed in Fig. 13.

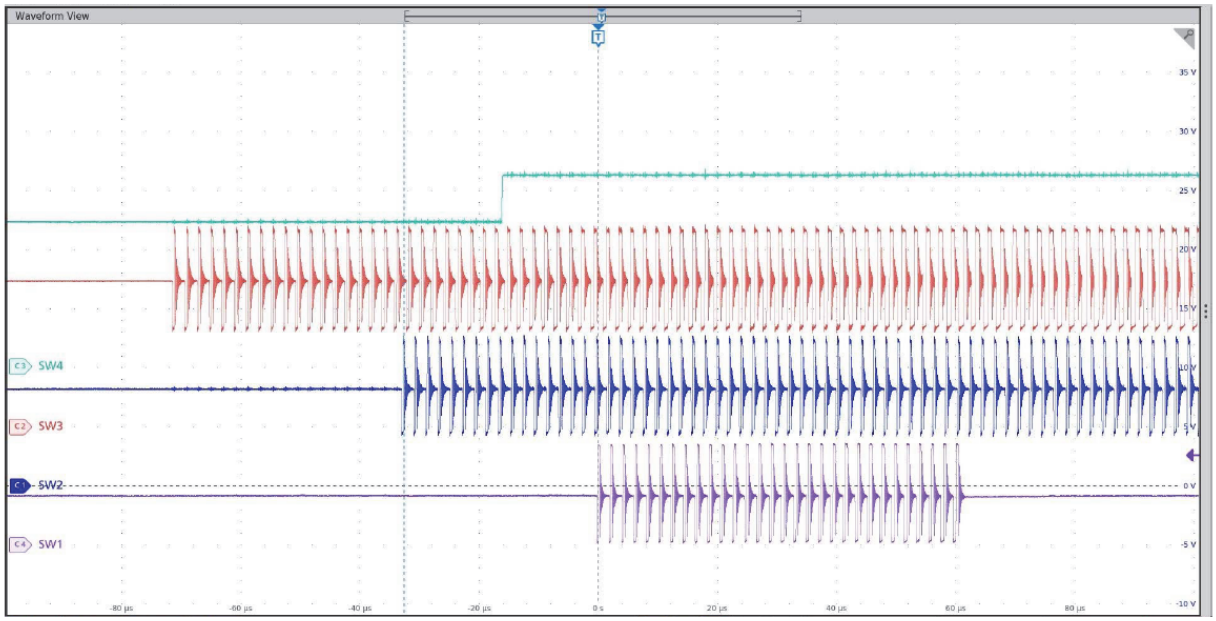

Fig. 14 – Measured waveforms for the series-connected cells during the charging and balancing phases.

It consists of the SEPIC converter, along with the current limiting circuit, three active cell-balancing circuits and one passive cell-balancing circuit. As in simulation, the charging current was 300 mA, but other tests run at 900 mA showed similar results.

During charging and balancing phases, the voltage across each of the four cells, as well as the switching signals (SW1, SW2, SW3 and SW4) for each of the balancing circuits were monitored using both the oscilloscope and a multimeter, with the resulting waveforms being presented in Fig. 14.

As expected, depending on the charging level of each lithium-ion cell, its corresponding balancing circuit alternatively enables and disables the switching regulator (or the MOSFET used for the passive circuitry) for a certain period of time, similar to the simulated circuit.

Regarding the efficiency of the circuitry, assuming that the output of each boost converter has about twice the magnitude of the input voltage and its efficiency is around 85 %, at a deflected current of around 200 mA (because just a part of the charging current is redistributed), this means that the overall power loss for each active cell-balancing circuit is 250 mW, compared to 1.66 W, for the passive cell-balancing circuit.

On the other hand, by applying this proposed architecture on a large number of series-connected cells, the overall efficiency of the entire balancing circuitry will be quite high because the 'bleeding' resistors will dissipate some amount of energy just for the last battery.

Depending on the desired charging current and the capacity of the entire battery pack, different switching regulators (featuring the most suitable peak current limit for a certain application and considering the characteristics of the boost topology) may be chosen, in order to ensure optimal balancing current for the cells.

5. CONCLUSIONS

This work presents the results of both simulation and practical implementation of a standalone analog active cell-balancing circuit intended for automotive BMSs, which offers the advantage of standalone usage, as well as the possibility of modularization and communication with several other devices.

The balancing circuitry which was designed for the series-connected lithium cells consists of three active circuits implemented using simple non-synchronous fixed frequency boost switching regulators (in contrast to [22], which proposes variable switching frequency control, that is more complex) and a passive 'bleeding' resistor-based circuit for the last cell from the top. The charging current for the entire string was set to 300 mA, while the voltage level for each cell was set to 4.15 V, with ±30 mV hysteresis.

In contrast to other architectures, the design proposed in this paper has the ability to balance the capacity of all cells both during charging and discharging phases, maximizing the reliability and the total amount of useful energy stored within the battery pack, while the efficiency of power conversion for the active circuits is around 85 %.

Depending on the targeted precision of the charging voltage (during the constant voltage phase) for each cell, dedicated comparators with integrated references can be used, in addition to the decrease of the hysteresis (from 60 mV to a lower value) which influences the maximum unbalance between the batteries.

For optimal balancing performances, the switching regulators should be chosen depending on their peak current limit (considering the characteristics of the boost converter topology), which should be correlated with the targeted charging current for the battery pack.

Apart from the automotive usage, active cell-balancing circuits for advanced lithium-ion batteries can also be developed for other industrial applications such as photovoltaic grids [23] or intelligent robotic systems [24], which may require high efficiency.

ACKNOWLEDGEMENTS

This work has been funded by University "Politehnica" of Bucharest, through the "Excellence Research Grants" Program, UPB – GEX 2017. Identifier: UPB – GEX2017, Ctr. No. 33/25.09.2017.

Received on June 26, 2018

REFERENCES

1. B. Anton, A. Florescu, *Matching the Performances of a Diesel Engine with a Mild-Hybrid Driving System, based on Telemetry Data*, 10th International Symposium on Advanced Topics in Electrical Engineering (ATEE), Bucharest, Romania, March 23-25, 2017.
2. B. Anton, A. Florescu, *Simple power management control for a plug-in mild-hybrid Diesel powertrain*, 9th International Conference on Electronics, Computers and Artificial Intelligence (ECAI), Targoviste, Romania, June 29-July 1, 2017.
3. L. Valda, K. Kosturik, *Comparison of Li-ion Active Cell Balancing Methods Replacing Passive Cell Balancer*, International Conference on Applied Electronics (AE), Pilsen, Czech Republic, Sept. 8-9, 2015.
4. S. Narayanaswamy, S. Steinhorst, M. Lukasiewycz, M. Kauer, S. Chakraborty, *Optimal Dimensioning of Active Cell Balancing Architectures*, Design, Automation & Test in Europe Conference & Exhibition (DATE), Dresden, Germany, March 24-28, 2014.
5. M. Lukasiewycz, M. Kauer, *Synthesis of Active Cell Balancing Architectures for Battery Packs*, IEEE Transactions on Computer-Aided Design of Integrated Circuits and Systems, **35**, *11*, pp. 1876–1889 (2016).
6. S. Steinhorst, M. Lukasiewycz, *Formal Approaches to Design of Active Cell Balancing Architectures in Battery Management Systems*, IEEE/ACM International Conference on Computer-Aided Design (ICCAD), Austin, TX, USA, Nov. 7-10, 2016.
7. M. Raber, D. O. Abdeslam, A. Heinzelmann, A. Ramirez, *Performance estimation of a cell-to-cell-type active balancing circuit for lithium-ion battery systems*, IEEE 26th International Symposium on Industrial Electronics (ISIE), Edinburgh, UK, June 19-21, 2017.
8. K. M. Lee, S. W. Lee, Y. G. Choi, B. Kang, *Active Balancing of Li-Ion Battery Cells Using Transformer as Energy Carrier*, IEEE Transactions on Industrial Electronics, **64**, *2*, pp. 1251–1257 (2017).
9. S. Jeon, J. J. Yun, S. Bae, *Active Cell Balancing Circuit for Series-connected Battery Cells*, 9th International Conference on Power Electronics and ECCE Asia (ICPE-ECCE Asia), Seoul, South Korea, June 1-5, 2015.
10. G. H. Min, J. I. Ha, *Active Cell Balancing Algorithm for Serially Connected Li-Ion Batteries based on Power to Energy Ratio*, IEEE Energy Conversion Congress and Exposition (ECCE), Cincinnati, OH, USA, Oct. 1-5, 2017.
11. N. Dahan, M. M. Peretz, I. Zeltser, *Cell-Level Hybrid Architectures for Active Balancing of Serially-Connected Batteries*, IEEE Applied Power Electronics Conference and Exposition (APEC), Tampa, FL, USA, March 26-30, 2017.
12. M. Kauer, S. Narayanaswamy, S. Steinhorst, M. Lukasiewycz, S. Chakraborty, *Many-to-Many Active Cell Balancing Strategy Design*, 20th Asia and South Pacific Design Automation Conference, Chiba, Japan, Jan. 19-22, 2015.
13. K. M. Lee, Y. C. Chung, C. H. Sung, B. Kang, *Active Cell Balancing of Li-Ion Batteries Using LC Series Resonant Circuit*, IEEE Transactions on Industrial Electronics, **62**, *9*, pp. 5491–5501 (2015).
14. N. Shivaraman, A. Easwaran, S. Steinhorst, *Efficient Decentralized Active Balancing Strategy for Smart Battery Cells*, Design, Automation & Test in Europe Conference & Exhibition (DATE), Lausane, Switzerland, March 27-31, 2017.

"Politehnica" University of Bucharest, Faculty of Electronics, Telecommunications and Information Technology, Bd. Iuliu Maniu, Nr. 1-3, Sector 6, Romania., bogdan_anton_2005@yahoo.com

15. A. Buturuga, D. Stoichescu, R. Constantinescu, *Universal system for automation of small tasks*, International Symposium of Fundamentals of Electrical Engineering (ISFEE), Bucharest, Romania, June 30-July 2, 2016.
16. R. Tahboub, R. Constantinescu, V. Lazarescu, C. Radoi, *Simulation results for secure automatic energy meter reading using mobile agents* (*Part 1*), Rev. Roum. Sci. Techn. – Electrotech. et Energ., **53**, *1*, pp. 75–86 (2008).
17. L. A. Perisoara, D. I. Sacaleanu, A. Vasile, *Instrument Clusters for Monitoring Electric Vehicles*, IEEE 23rd International Symposium for Design and Technology in Electronic Packaging (SIITME), Constanta, Romania, Oct. 26-28, 2017.
18. L. A. Perisoara, A. Vasile, D. I. Sacaleanu, *Vehicles diagnosis based on LabVIEW and CAN interfaces*, IEEE 23rd International Symposium for Design and Technology in Electronic Packaging (SIITME), Constanta, Romania, Oct. 26-28, 2017.
19. Y. Barsukov, J. Qian, *Battery Power Management for Portable Devices*, Artech House, 2013, pp. 125–138.
20. R. Erickson, D. Maksimovic, *Fundamentals of Power Electronics*, Second edition, Kluwer Academic Publishers New York, Boston, Dordrecht, London, Moscow, 2004, pp. 22–27.
21. A. Rahmoun, H. Biechl, *Modelling of Li-ion batteries using equivalent circuit diagrams*, Electrical Review, **88**, *7*, pp. 152–156 (2012).
22. S. W. Lee, Y. G. Choi, S. W. Bae, J. J. Yun, *A New Variable Switching Frequency Control for Active Cell Balancing Systems*, IEEE International Conference on Consumer Electronics (ICCE), Las Vegas, NV, USA, Jan. 8-10, 2017.
23. C. Lupu, A. Petrescu-Nita, C. Petrescu, M. Lupu, *Design consideration on algorithms and control structures for photovoltaic grids*, 19th International Conference on System Theory, Control and Computing (ICSTCC), Cheile Gradistei, Romania, Oct. 14-16, 2015.
24. A. M. Stanescu, A. Nita, M. A. Moisescu, I. S. Sacala, *From industrial robotics towards intelligent robotic systems*, 4th International IEEE Conference Intelligent Systems, Varna, Bulgaria, Sept. 6-8, 2008.